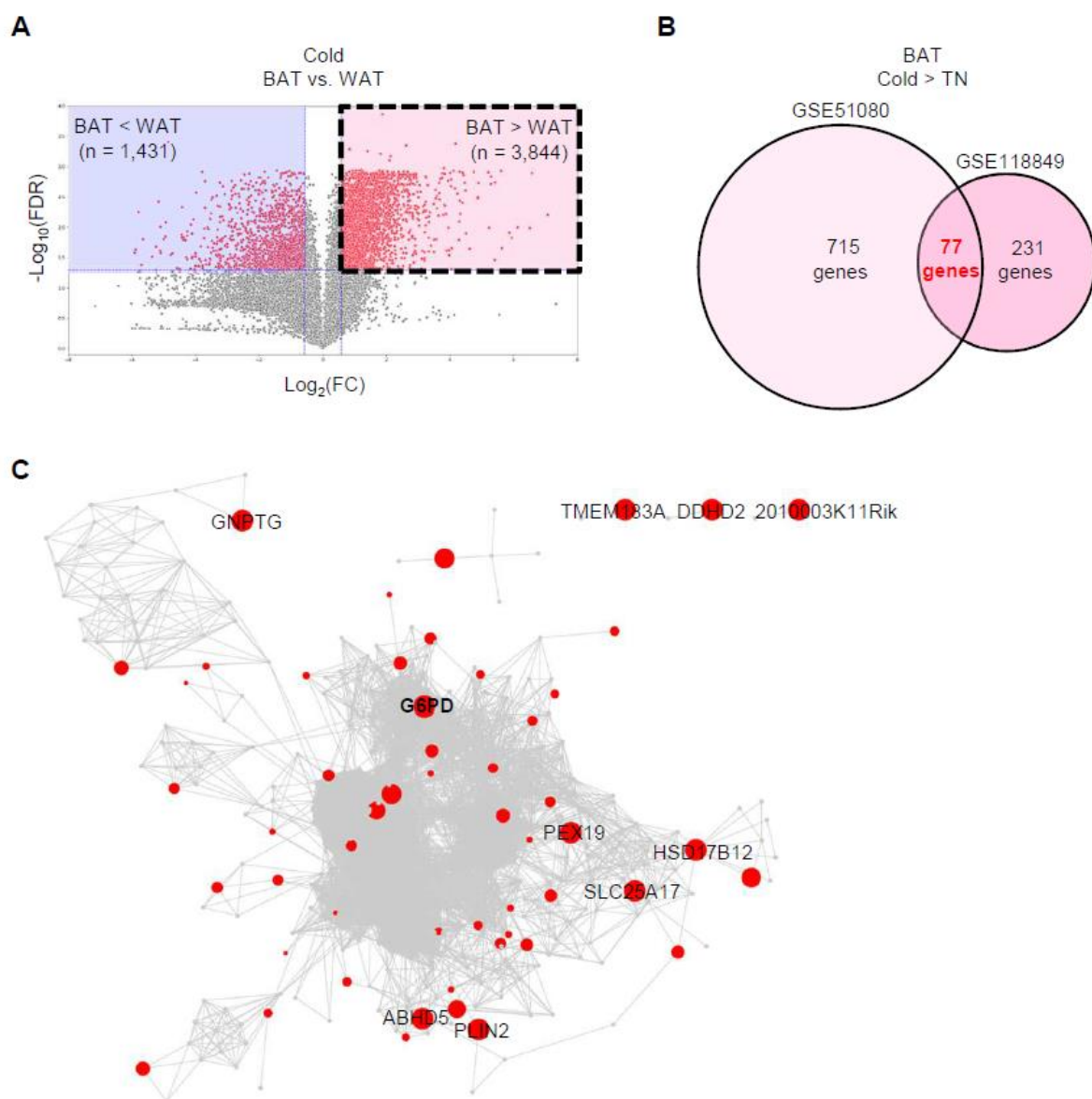


SUPPLEMENTARY DATA

Spatial Regulation of Reactive Oxygen Species via G6PD in Brown Adipocytes Supports Thermogenic Function

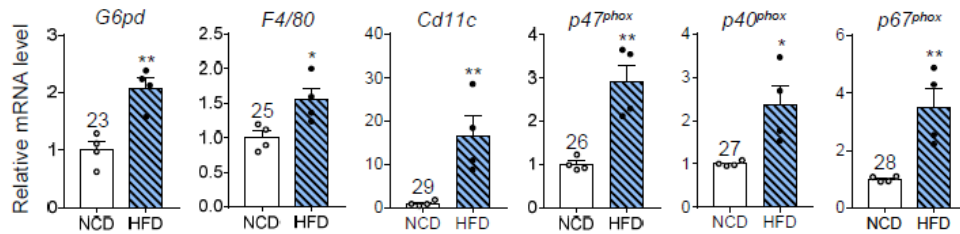
Jee Hyung Sohn, Yul Ji, Chang-Yun Cho, Hahn Nahmgoong, Sangsoo Lim, Yong Geun Jeon, Sang Mun Han, Ji Seul Han, Isaac Park, Hyun-Woo Rhee, Sun Kim and Jae Bum Kim

Supplementary Figure 1. Bioinformatics analyses of genes enriched in BAT and increased by cold stimulation. A: Differentially expressed genes identified with $FC \geq 1.4$ and $FDR < 0.05$ cut-off. B: Identification of 77 candidate genes which are commonly upregulated upon cold stimulation in BAT using two microarray data set. Candidate genes were screened using FC value and FDR at the thresholds ($FC \geq 1.4$ and $FDR < 0.05$). C: PPI subnetwork containing genes in the top 5% of the NP score. Red dots and grey dots indicate candidate genes and genes affected by candidate genes, respectively. Node size represents NP score.

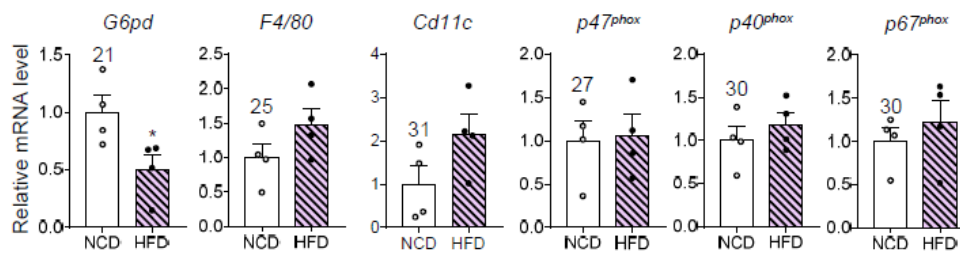


Supplementary Figure 2. The mRNA levels of *G6pd*, inflammation- and oxidation-related genes in eWAT and BAT from obese mice. A: The mRNA levels of *G6pd*, pro-inflammatory genes and pro-oxidative genes in eWAT and BAT from 8w HFD-fed mice compared with NCD-fed mice. B: The mRNA levels of *G6pd*, pro-inflammatory genes and pro-oxidative genes in eWAT and BAT from *db/db* mice compared to *db/+* mice. All data represent the mean \pm SEM. All qRT-PCR data were normalized to the mRNA level of *Ppia*. * $p < 0.05$, ** $p < 0.01$ vs. each control group by Student's *t*-test. The cycle threshold value for each control group is indicated.

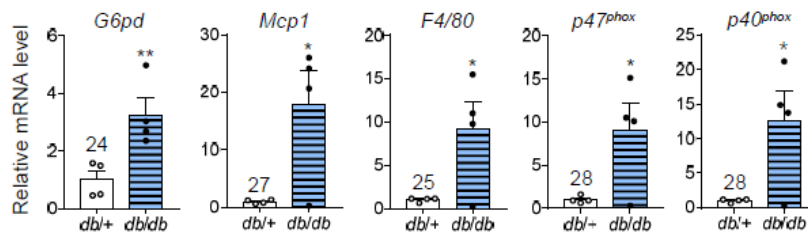
A (i) eWAT



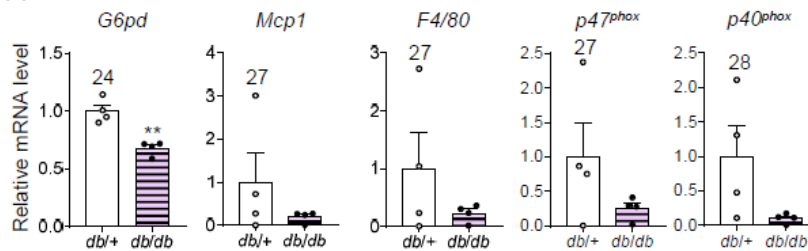
(ii) BAT



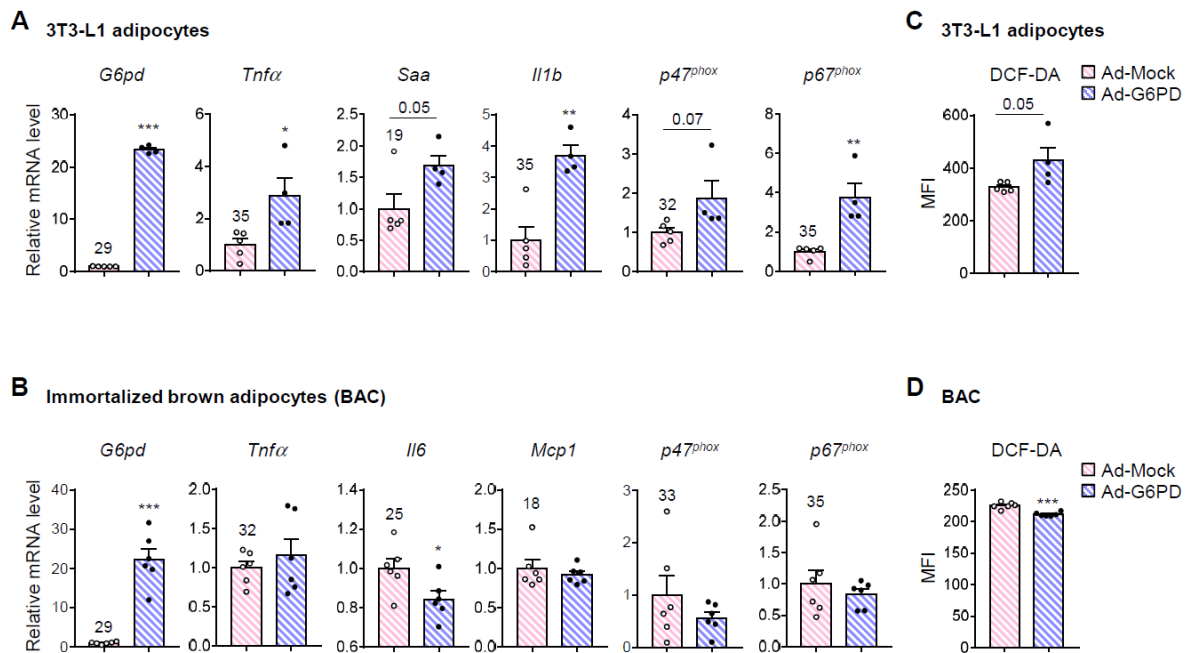
B (i) eWAT



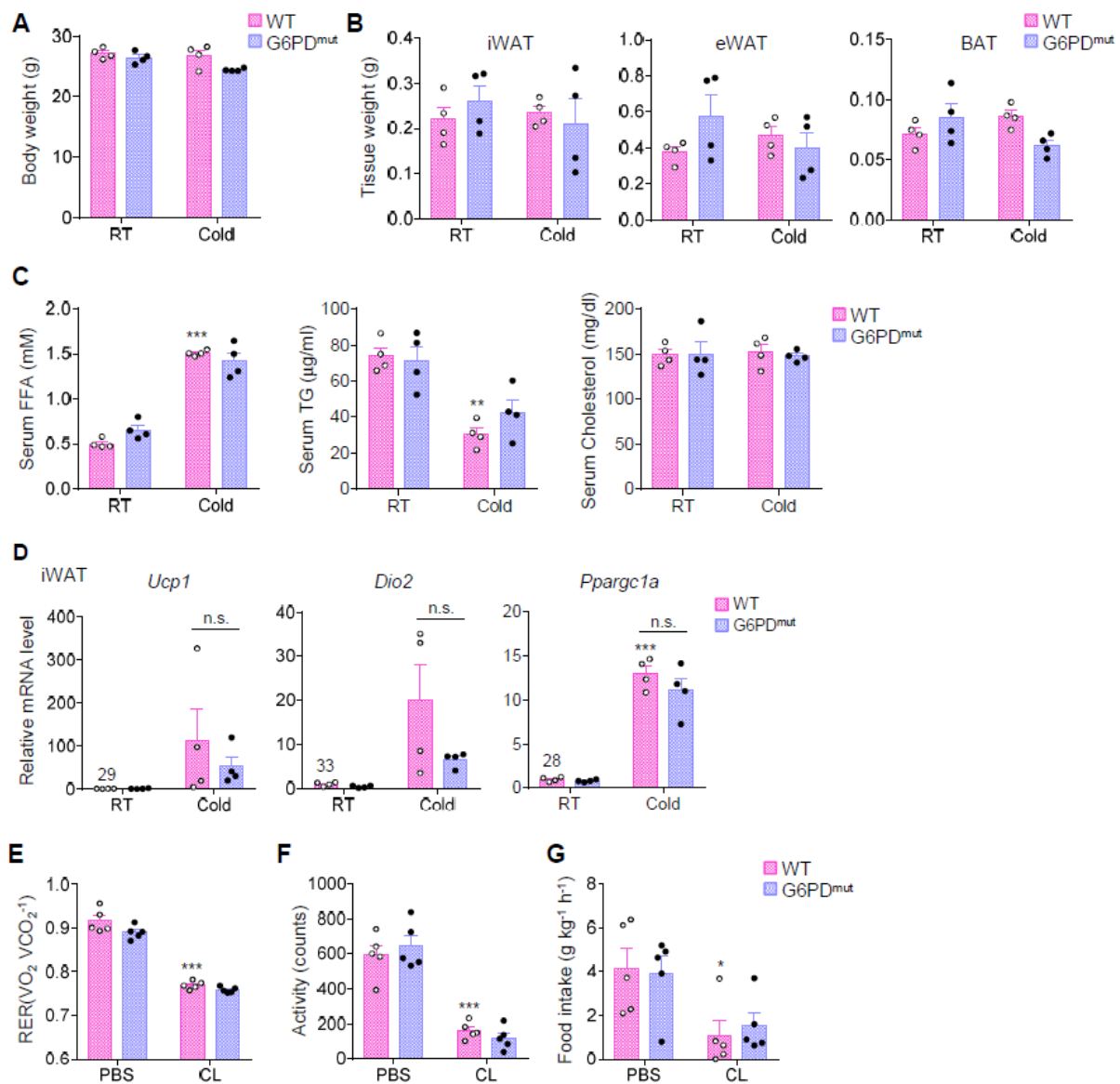
(ii) BAT



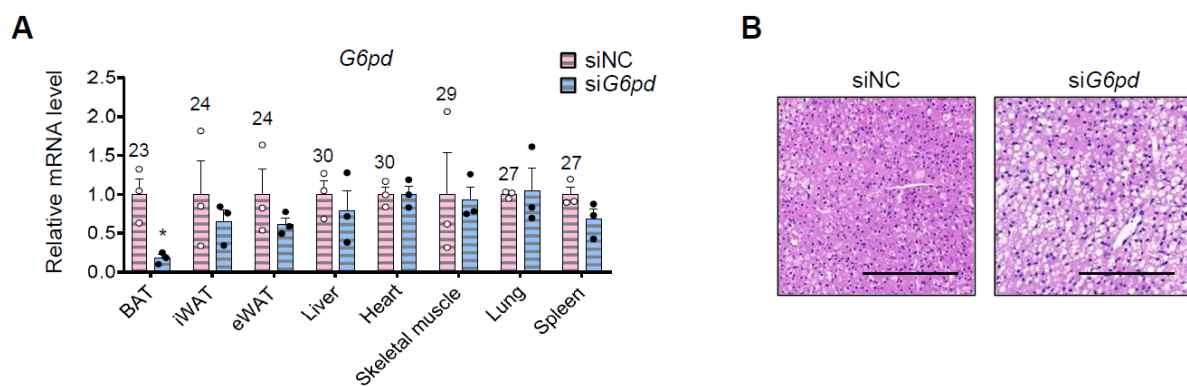
Supplementary Figure 3. The mRNA levels of inflammatory and oxidative genes in white and brown adipocytes upon G6PD overexpression. A and B: The mRNA levels of pro-inflammatory genes and NADPH oxidase subunits in 3T3-L1 adipocytes (A) or immortalized mouse brown adipocytes (BAC) (B) with G6PD overexpression using adenovirus. C and D: Cellular ROS level in 3T3-L1 adipocytes (C) or BAC (D) with G6PD overexpression. All data represent the mean \pm SEM. All qRT-PCR data were normalized to the mRNA level of *Ppia*. * $p < 0.05$, ** $p < 0.01$, *** $p < 0.001$ vs. Ad-Mock group by Student's *t*-test. The cycle threshold value for each control group is indicated.



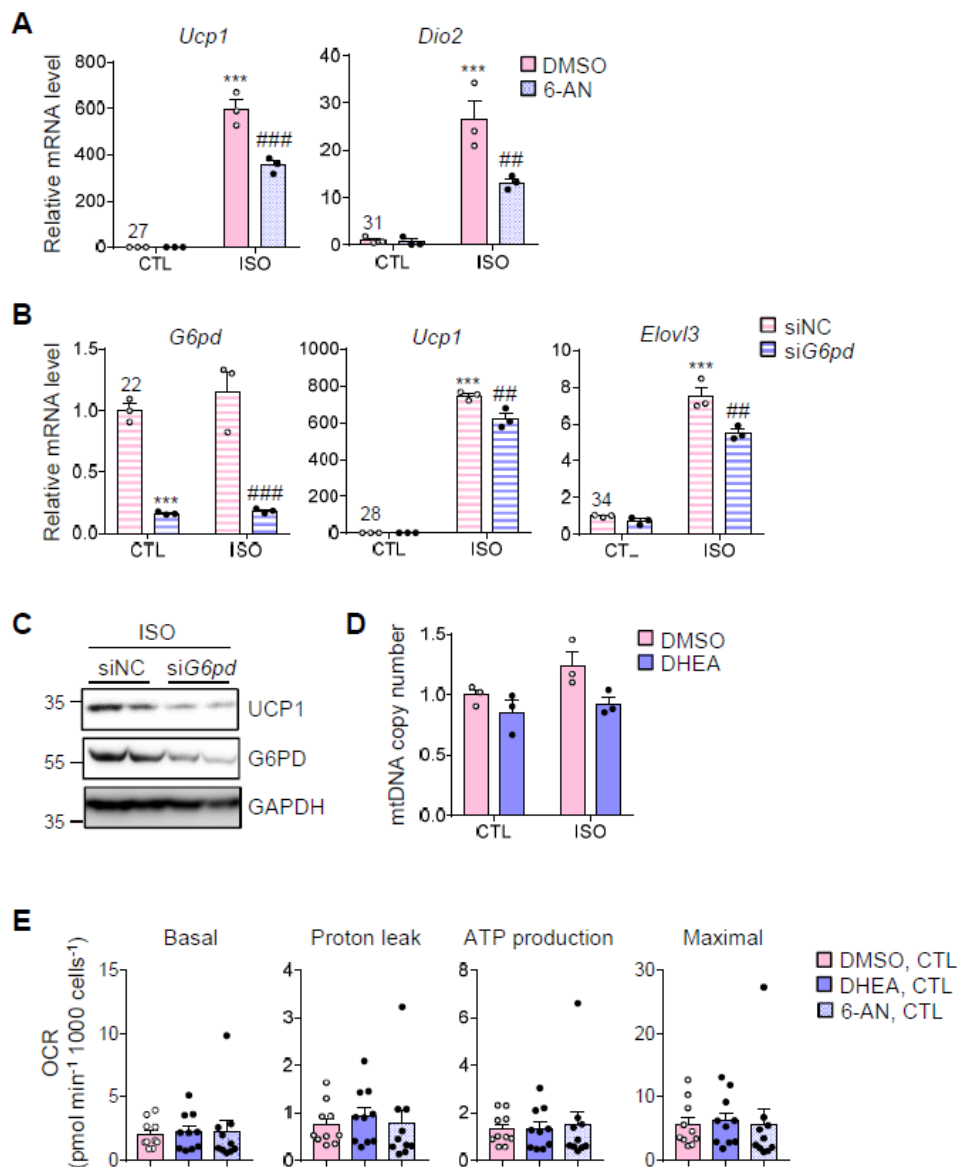
Supplementary Figure 4. The phenotypes of WT and G6PD^{mut} mice upon cold exposure and β -adrenergic stimulation. A and B: Body weight (A) and adipose tissue weights (B) from WT and G6PD^{mut} mice exposed to RT or 6 h cold condition. C: Serum lipid profile of WT and G6PD^{mut} mice upon 6 h cold exposure. ** $p < 0.01$, *** $p < 0.001$ vs. WT, RT group by two-way ANOVA followed by Tukey's post-hoc test. D: The mRNA levels of thermogenic marker genes in iWAT of WT and G6PD^{mut} mice during 6 h cold exposure. qRT-PCR data were normalized to the mRNA level of *36b4*. *** $p < 0.001$ vs. WT, RT group. E–G: Respiratory exchange ratio (RER) (E), physical activity (F), and food intake (G) of WT and G6PD^{mut} mice before and after CL (1 mg/kg body weight) injection were determined. * $p < 0.05$, *** $p < 0.001$ vs. WT, PBS group. All data represent the mean \pm SEM. The cycle threshold value for each control group is indicated. n.s., not significant.



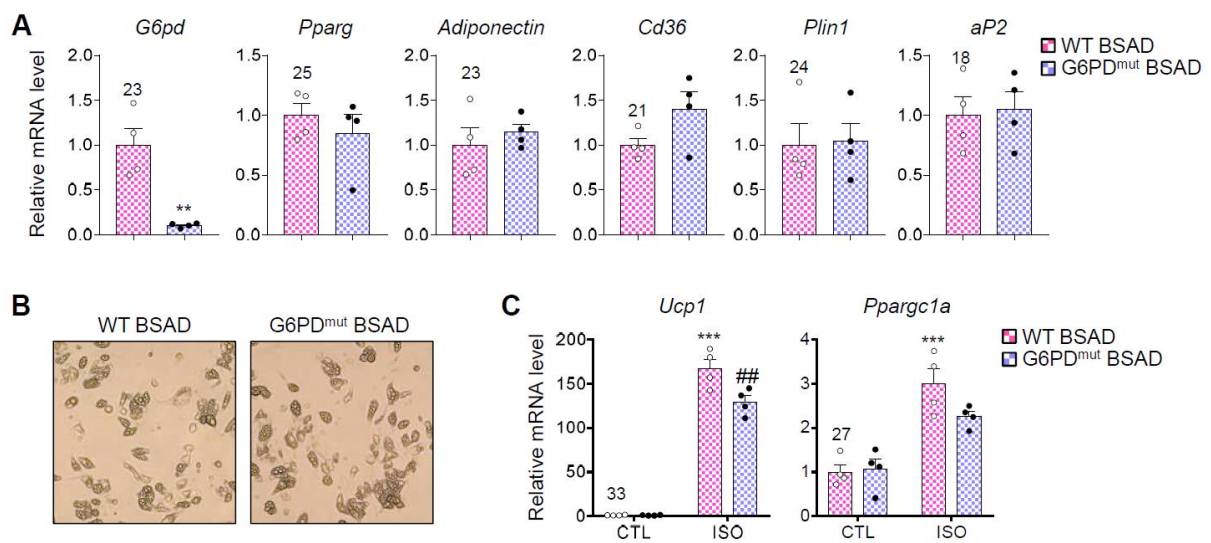
Supplementary Figure 5. The phenotypes of BAT-specific G6PD-suppressed mice after cold exposure. A: Tissue distribution of *G6pd* mRNA expression in BAT-specific siRNA-treated WT mice exposed to 6 h cold condition. B: Adipocyte morphology of BAT as assessed by H&E staining. Scale bars, 200 μ m. qRT-PCR data were normalized to the mRNA level of *36b4*. * $p < 0.05$ vs. siNC group by Student's *t*-test. All data represent the mean \pm SEM. The cycle threshold value for each control group is indicated.



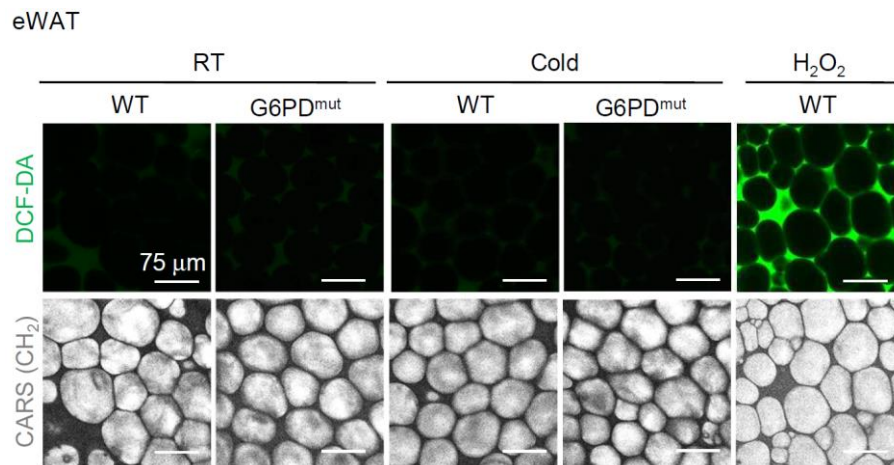
Supplementary Figure 6. In brown adipocytes, thermogenic gene expression and mitochondrial oxygen consumption rates upon G6PD suppression. A: Differentiated BAC was pretreated with G6PD inhibitor, 100 μ M 6-AN for 2 h. Relative mRNA levels of thermogenic genes in BAC without or with 1 μ M ISO treatment for 3 h as measured by qRT-PCR. *** P < 0.001 vs. DMSO, CTL group; ## P < 0.01, ### P < 0.001 vs. DMSO, ISO group by two-way ANOVA followed by Tukey's post-hoc test. B and C: Thermogenic gene expressions (B) and UCP1 protein levels (C) in brown adipocytes transfected with siNC or si*G6pd*. *** p < 0.001 vs. siNC, CTL group; ## p < 0.01, ### p < 0.001 vs. siNC, ISO group by two-way ANOVA followed by Tukey's post-hoc test. qRT-PCR data were normalized to the mRNA level of *Ppia*. The cycle threshold value for each control group is indicated. D and E: Mitochondrial DNA (mtDNA) contents (mtDNA/nuclear DNA ratio) upon ISO treatment (D) and OCRs in the absence of ISO (E) in brown adipocytes upon G6PD inhibition. All data represent the mean \pm SEM.



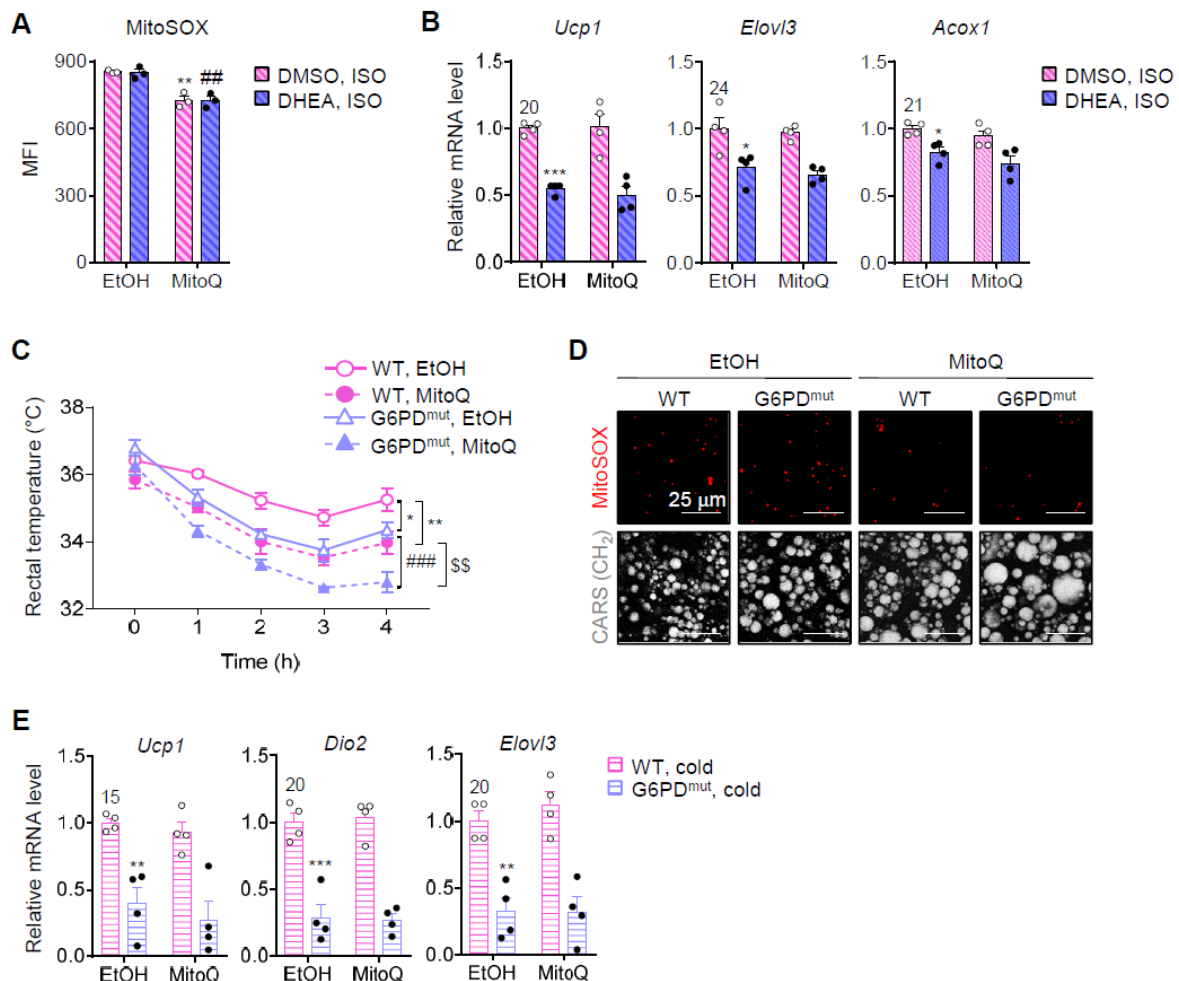
Supplementary Figure 7. In SVC-derived brown adipocytes, expression levels of adipogenic and thermogenic genes upon G6PD deficiency. A–C: Adipogenic gene expression levels (A), adipocyte morphology ($\times 200$ magnification) (B), and mRNA levels of thermogenic genes (C) in BSAD. $***p < 0.001$ vs. WT, CTL group; $##p < 0.01$ vs. WT, ISO group by two-way ANOVA followed by Tukey's post-hoc test. qRT-PCR data were normalized to the mRNA level of *Ppia*. The cycle threshold value for each control group is indicated. All data represent the mean \pm SEM.



Supplementary Figure 8. Cellular ROS level in eWAT from G6PD^{mut} mice. Cellular ROS level in eWAT from WT and G6PD^{mut} mice upon cold exposure as measured DCF-DA staining. Scale bars, 75 μ m.

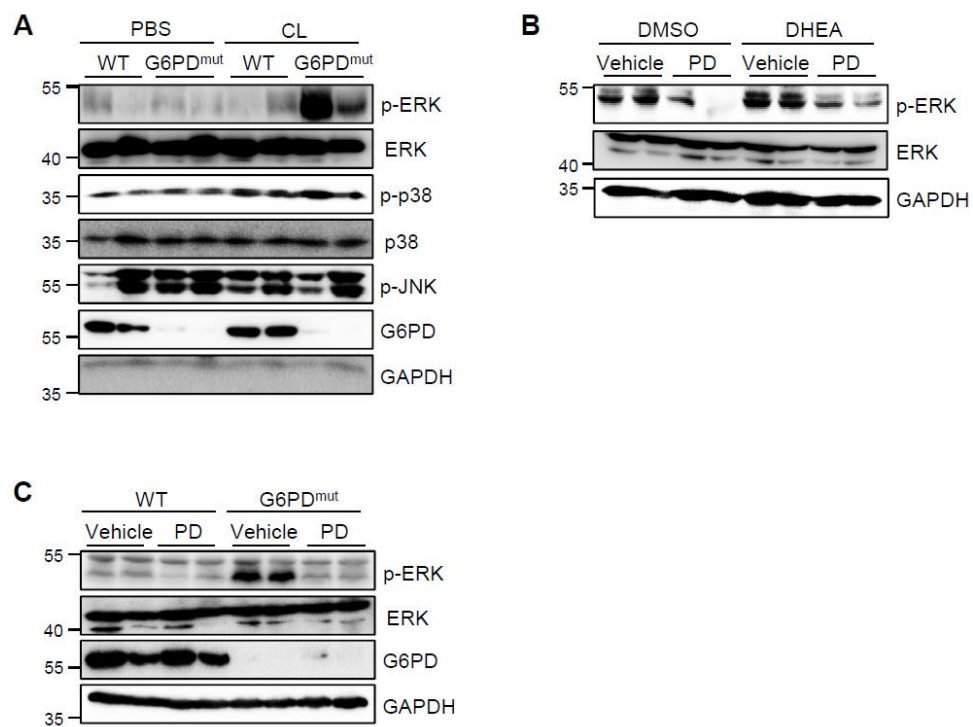


Supplementary Figure 9. The effects of mitochondrial ROS scavenger on G6PD-deficient brown adipocytes. A and B: The levels of mitochondrial superoxide (A) and thermogenic gene expression (B) in G6PD-inhibited brown adipocytes upon 100 nM MitoQ treatment in the presence of ISO. BAC were pretreated with 100 μ M DHEA and 100 nM MitoQ for 2 h, followed by 1 μ M ISO treatment for 3 h. * p < 0.05, ** p < 0.01, *** p < 0.001 vs. DMSO, ISO, EtOH group; ## p < 0.01 vs. DHEA, ISO, EtOH group by two-way ANOVA followed by Tukey's post-hoc test. C: Rectal temperature of WT and G6PD^{mut} mice upon MitoQ injection (5 mg/kg body weight) followed by cold exposure. MitoQ was i.p. injected into WT or G6PD^{mut} mice. After 10 min, mice were exposed to cold condition for 4 h. * p < 0.05, ** p < 0.01 vs. WT, EtOH group; ### p < 0.001 vs. G6PD^{mut}, EtOH group; \$\$ p < 0.01 vs. WT, MitoQ group by RM-ANOVA followed by Tukey's post-hoc test. D and E: The levels of mitochondrial ROS (D) and thermogenic gene expressions (E) in BAT of G6PD^{mut} mice upon MitoQ injection. Scale bars, 25 μ m. ** p < 0.01, *** p < 0.001 vs. WT, cold, EtOH group by two-way ANOVA followed by Tukey's post-hoc test. All data represent the mean \pm SEM. qRT-PCR data were normalized to the mRNA level of *Ppia*. The cycle threshold value for each control group is indicated.

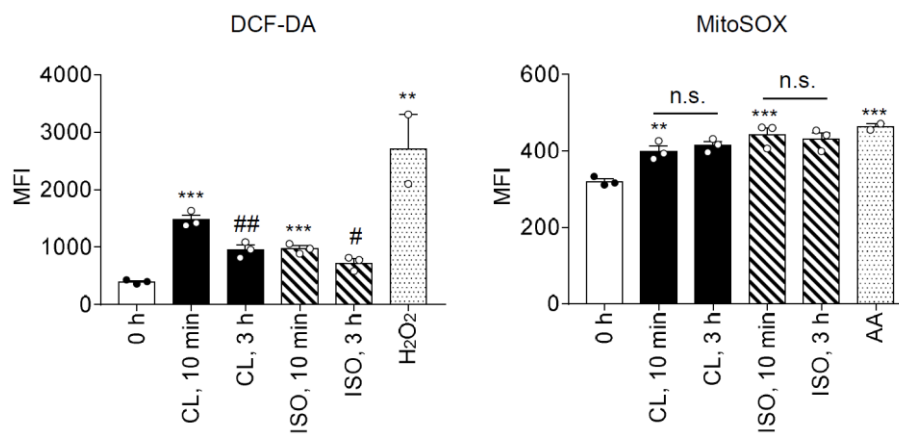


Supplementary Figure 10. ROS-induced ERK activation in brown adipocytes upon G6PD defect.

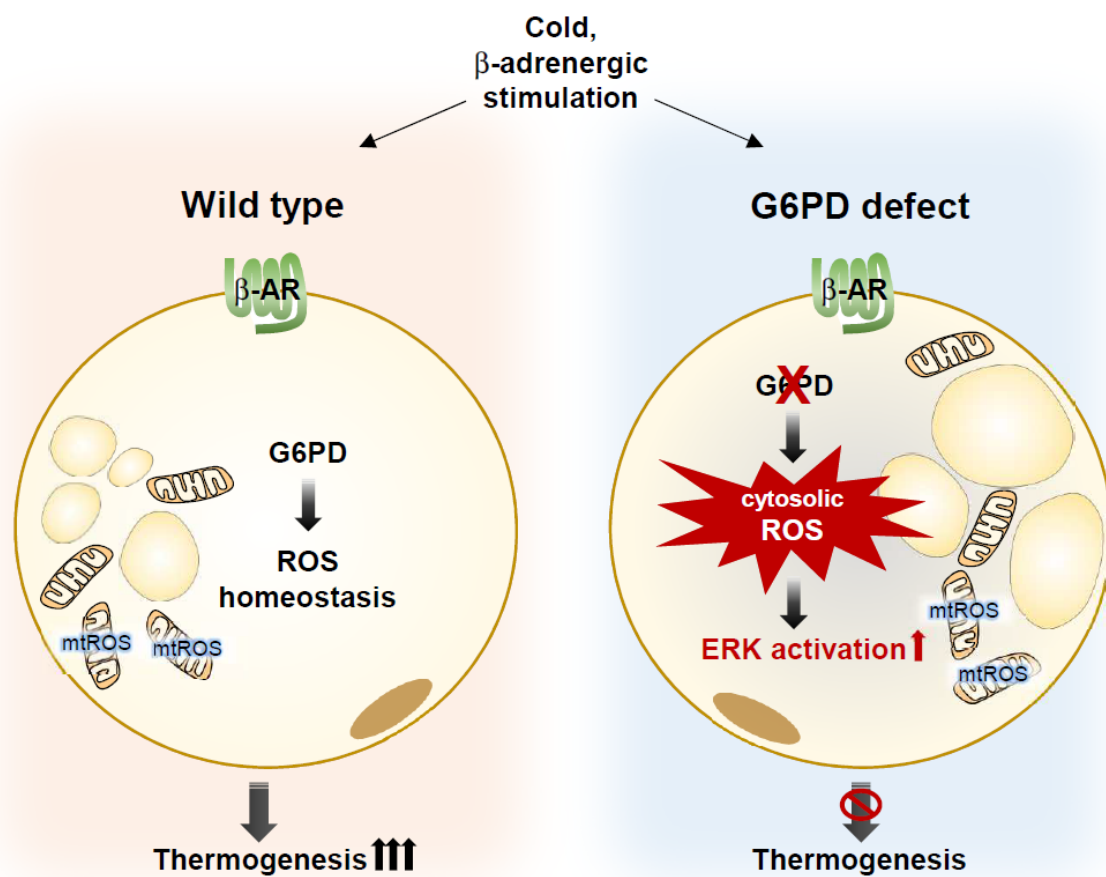
A: MAPK activation in BAT from WT and G6PD^{mut} mice after 4 h CL (1 mg/kg body weight) injection.
B and C: The level of ERK phosphorylation in DHEA-treated brown adipocytes (B) or BAT of G6PD^{mut} mice (C) upon PD treatment.



Supplementary Figure 11. Cellular ROS and mitochondrial ROS level upon β -adrenergic stimulation. Cellular ROS and mitochondrial superoxide level in BAC upon CL (2.5 μ M) and ISO (5 μ M) treatment as measured DCF-DA and mitoSOX staining. All data represent the mean \pm SEM. ** $p < 0.01$, *** $p < 0.001$ vs. 0 h group; # $p < 0.05$, ## $p < 0.01$ vs. each stimuli, 10 min group by one-way ANOVA followed by Tukey's post-hoc test. n.s., not significant; AA, antimycin A.



Supplementary Figure 12. Proposed model. In G6PD-deficient brown adipocytes, cytosolic ROS accumulation provokes ERK activation under cold or β -adrenergic stimulation, contributing to impairment of thermogenic program.



Supplementary Table 1. Oligo sequences for siRNA

Gene	Forward	Reverse
mouse G6pdx	GUCAACCUCAUCCCACCUA	UAGGUGGGAUGAGGUUGAC
Negative control	AAACAAGCCCAUUCGCGGAUU	AAUCCGCGAAUGGGCUUGUUU

Supplementary Table 2. Primers used for qRT-PCR and mtDNA/genomic DNA ratio

Gene	Forward	Reverse
mouse G6pdx	GATCTGTGAACGTGTTTGGC	TGTGTGTATCAGCTTGGTGG
mouse Ucp1	CTTTGCCTCACTCAGGATTGG	ACTGCCACACCTCCAGTCATT
mouse Dio2	CAGTGTGGTGCACGTCTCCAATC	TGAACCAAAGTTGACCACCAG
mouse Ppargc1a	CCCTGCCATTGTTAAGACC	TGCTGCTGTTCTGTTTTTC
mouse Elvol3	ATGCAACCCTATGACTTCGAG	ACGATGAGCAACAGATAGACG
mouse Cidea	GCCGTGTTAAGGAATCTGCTG	TGCTCTTCTGTATCGCCCAGT
mouse Acox1	CAGGAAGAGCAAGGAAGTGG	CCTTTCTGGCTGATCCCATA
mouse Ppia	CAGACGCCACTGTGCGTTT	TGTCTTTGGAACCTTGTCTGCAA
mouse Mcp1	AGGTCCCTGTCATGCTTCTG	TCTGGACCCATTCTTCTTG
mouse Tnfa	CGGAGTCCGGGCAGGT	GCTGGGTAGAGAATGGATGAACA
mouse Il-6	AGTTGCCTTCTTGGGACTGA	TCCACGATTTCCAGAGAAC
mouse F4/80	GCTGCACCTCTGTGCCTTT	CAGGTATGCCATGATGCTTG
mouse Cd11c	GAGGATTTGAGCATCCCAGA	CACCTGCTCCTGACACTCAA
mouse p47phox	GATGTTCCCCATTGAGGCCG	GTTTCAGGTCATCAGGCCGC
mouse p67phox	CTGGCTGAGGCCATCAGACT	AGGCCACTGCAGAGTGCTTG
mouse p40phox	GCCGCTATCGCCAGTTCTAC	GCAGGCTCAGGAGGTTCTTC
mouse Il-1b	TGCAGAGTTCCCCAACTGGTACATC	GTGCTGCCTAATGTCCCCTTGAATC
mouse Saa	AGCGATGCCAGAGAGGCTGT	ACCCAGTAGTTGCTCCTCTT
mouse 36b4	GCTCCAAGCAGATGCAGCA	CCGGATGTGAGGCAGCAG
mouse Srebp1c	GGAGCCATGGATTGCACATT	CAGGAAGGCTTCCAGAGAGG
mouse Scd1	CCGGAGACCCCTTAGATCGA	TAGCCTGTAAAGATTTCTGCAAACC
mouse Fasn	GCCTACACCCAGAGCTACCG	GCCATGGTACTTGGCCTTG
mouse 16s rRNA	ACATCCAATGGTGTAGAAG	AAGTTGAGAGCGCTTATTTG
mouse 18s rRNA	CGCGGTTCTATTTTGTGGT	AGTCGGCATCGTTTATGGTC

Supplementary Table 3. NP score and degree centrality transition of candidate genes in BAT upon cold exposure

Gene	GSE118849_FC	NP_score	FC rank	NP_score rank	Degree of centrality in template network	Degree of centrality in sub network
Ddhd2	4.049205	0.526316	31	1	7.32E-05	0.001459854
2010003K11Rik	3.822729	0.526316	34	1	7.32E-05	0.001459854
Tmem183a	1.535835	0.526316	61	1	7.32E-05	0.001459854
Hsd17b12	3.891745	0.344511	33	4	0.001538	0.026277372
Gnptg	1.840352	0.22231	56	5	0.000146	0.002919708
Abhd5	3.0354	0.166214	41	6	0.000366	0.00729927
Pex19	2.261019	0.163793	47	7	0.001392	0.020437956
Slc25a17	4.627142	0.155804	23	8	0.000293	0.005839416
Plin2	4.42553	0.153653	26	9	0.00022	0.004379562
G6pdx	3.155075	0.142841	38	10	0.003076	0.056934307
Lrrc8d	5.56786	0.138544	20	11	0.000146	0.002919708
Acly	6.72252	0.138348	14	12	0.010986	0.2
Hacd2	7.445061	0.137755	11	13	0.000146	0.002919708
Mgll	4.064763	0.13335	30	14	0.002563	0.011678832
Orm1	2.035206	0.133329	51	15	0.018163	0.21459854
Pigq	6.477094	0.125311	17	16	0.001025	0.018978102
Letm1	6.57685	0.124852	16	17	0.00022	0.004379562
Acox2	5.316918	0.124229	21	18	0.004907	0.083211679
Rbks	1.997121	0.122756	52	19	0.000879	0.017518248
Pfkfb	6.587111	0.12185	15	20	0.002344	0.039416058
Elovl3	140.7226	0.121775	1	21	0.00022	0.004379562
Retsat	4.18173	0.120872	29	22	0.001538	0.010218978
Gpd1	7.664313	0.120544	8	23	0.001099	0.017518248
Dhcr24	8.24017	0.12006	7	24	0.001465	0.020437956
Pgd	7.139776	0.119699	12	25	0.000732	0.013138686
Dpp7	3.097665	0.118501	39	26	0.007983	0.15620438
Sgcb	2.238766	0.11738	49	27	0.000732	0.01459854
Peli2	2.389573	0.117316	44	28	0.000293	0.005839416
Sgpl1	1.955796	0.117061	53	29	0.000659	0.010218978
Hebp2	3.075985	0.117015	40	30	0.007837	0.15620438
Pcca	3.462851	0.116398	36	31	0.002197	0.035036496
Adcy10	18.30422	0.116365	4	32	0.000806	0.002919708
Acot12	20.84364	0.113765	2	33	0.001392	0.023357664
Idh3a	2.493076	0.113755	43	34	0.00227	0.027737226
Cnnm2	7.498979	0.113279	10	35	7.32E-05	0.001459854
Abhd6	1.701766	0.112499	59	36	0.002051	0.004379562
Mtor	5.976586	0.112363	19	37	0.007031	0.018978102
Ube2f	2.08759	0.112119	50	38	0.021386	0.037956204
Ncan	7.569822	0.111649	9	39	0.000146	0.002919708
Nudt1	2.259429	0.111391	48	40	7.32E-05	0.001459854
Fah	6.776479	0.111244	13	41	0.000806	0.010218978
Pafah2	4.235276	0.10917	28	42	0.000659	0.011678832
Mlec	2.34439	0.108272	45	43	0.00769	0.058394161
Uck2	3.642462	0.10811	35	44	0.001172	0.010218978
Pak1ip1	1.715852	0.107599	58	45	0.006006	0.002919708
Vps53	1.658851	0.107417	60	46	0.00293	0.023357664
Fbxl2	4.459444	0.107308	25	47	0.001099	0.016058394
Socs5	1.908951	0.107084	54	48	0.012011	0.026277372
Cux1	6.110062	0.106928	18	49	0.001904	0.017518248
Atp6v0a2	3.448155	0.106855	37	50	0.002344	0.011678832
Rbsn	1.718759	0.105609	57	51	0.001025	0.004379562
St3gal5	9.688721	0.105403	6	52	0.000513	0.010218978
Pdcd6ip	1.854537	0.105106	55	53	0.000513	0.008759124
Rnf185	2.279728	0.105016	46	54	0.000146	0.002919708
Egln1	4.805963	0.104589	22	55	0.00498	0.018978102
Ptk2b	4.340295	0.104247	27	56	0.003003	0.008759124
Acot11	14.08509	0.103368	5	57	7.32E-05	0.001459854
Grk3	2.649235	0.103307	42	58	0.000732	0.010218978
Sorl1	20.06046	0.102353	3	59	0.000439	0.008759124
Vwa8	4.498722	0.101	24	60	0.000146	0.002919708
Tbc1d20	4.038552	0.100476	32	61	0.000146	0.002919708

* Among candidate genes, 16 genes did not exceed the threshold (800 combined scores).

Supplementary Video 1. Body temperature of WT and G6PD^{mut} mice after cold exposure. Thermal infrared imaging of live mice after 4 h cold exposure, related to Fig. 3B.

Supplementary Video 2. Body temperature of mice with BAT-specific G6PD downregulation. BAT from WT were injected with siNC or si*G6pd* (20 µg/mouse), followed by cold exposure. After 4 h, body temperature of live mice were analyzed by thermal infrared camera, related to Fig. 3J.

Supplementary Video 3. Body temperature of WT and G6PD^{mut} mice injected with PBS or NAC. WT and G6PD^{mut} mice were i.p. injected with PBS or NAC (100 mg/kg body weight), followed by CL (0.5 mg/kg body weight) administration. After 20 min, surface body temperatures of live mice were analyzed by thermal infrared camera, related to Fig. 6H.

Supplementary Video 4. Body temperature of WT and G6PD^{mut} mice injected with vehicle or PD. WT and G6PD^{mut} mice were i.p. injected with vehicle or PD (10 mg/kg body weight), followed by cold exposure. After 4 h, body temperature of live mice were analyzed by thermal infrared camera, related to Fig. 7D.